ACCOUNTS
of chemical research

Wet Chemical Functionalization of Graphene

ANDREAS HIRSCH,* JAN M. ENGLERT, AND FRANK HAUKE

Department of Chemistry and Pharmacy and Institute of Advanced Materials and Processes (ZMP), University of Erlangen-Nürnberg, Henkestrasse 42, 91054 Erlangen, Germany

RECEIVED ON APRIL 26, 2012

CONSPECTUS

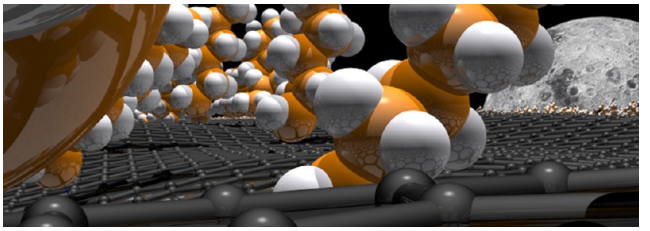

The fullerenes, carbon nanotubes, and graphene have enriched the family of carbon allotropes over the last few decades. Synthetic carbon allotropes (SCAs) have attracted chemists, physicists, and materials scientists because of the sheer multitude of their aesthetically pleasing structures and, more so, because of their outstanding and often unprecedented properties. They consist of fully conjugated p-electron systems and are considered topologically confined objects in zero, one, or two dimensions.

Among the SCAs, graphene shows the greatest potential for high-performance applications, in the field of nanoelectronics, for example. However, significant fundamental research is still required to develop graphene chemistry. Chemical functionalization of graphene will increase its dispersibility in solvents, improve its processing into new materials, and facilitate the combination of graphene's unprecedented properties with those of other compound classes.

On the basis of our experience with fullerenes and carbon nanotubes, we have described a series of covalent and noncovalent approaches to generate graphene derivatives. Using water-soluble perylene surfactants, we could efficiently exfoliate graphite in water and prepare substantial amounts of single-layer-graphene (SLG) and few-layer-graphene (FLG). At the same time, this approach leads to noncovalent graphene derivatives because it establishes efficient $\pi-\pi$-stacking interactions between graphene and the aromatic perylene chromophors supported by hydrophobic interactions.

To gain efficient access to covalently functionalized graphene we employed graphite intercalation compounds (GICs), where positively charged metal cations are located between the negatively charged graphene sheets. The balanced combination of intercalation combined with repulsion driven by Coulombic interactions facilitated efficient exfoliation and wet chemical functionalization of the electronically activated graphene sheets via trapping with reactive electrophilic addends. For example, the treatment of reduced graphite with aryl diazonium salts with the elimination of N_2 led to the formation of arylated graphene. We obtained alkylated graphene via related trapping reactions with alkyl iodides.

These new developments have opened the door for combining the unprecedented properties of graphene with those of other compound classes. We expect that further studies of the principles of graphene reactivity, improved characterization methods, and better synthetic control over graphene derivatives will lead to a whole series of new materials with highly specific functionalities and enormous potential for attractive applications.

Introduction

The family of carbon allotropes, which for a long time consisted of the natural forms of diamond and graphite only, has been enriched in the past few decades by the fullerenes, the carbon nanotubes, and graphene.[1−3] What makes synthetic carbon allotropes (SCAs) so attractive for chemists, physicists, and materials scientists is not only the sheer multitude of aesthetically pleasing structures[4] but, even more so, their outstanding and in many cases unprecedented properties.[5,6] They consist of fully conjugated π-electron systems and can be considered as topologically confined objects in 0-, 1-, or 2-dimensions, respectively. These extended electron reservoirs yield pronounced redox-activity and high electron mobility.[7] At the same time, SCAs are characterized by stability under ambient conditions. Indeed, metallic carbon nanotubes and graphene are the first representatives of stable organic metals, where no further activation by doping or charge

Published on the Web 09/04/2012 www.pubs.acs.org/accounts
10.1021/ar300116q

transfer is required to establish high charge-carrier mobility. For graphene, an almost temperature-independent charge-carrier mobility[7] of up to $\mu = 200\,000$ cm^2/(V s) in the suspended state and carrier concentrations of $n = 2 \times 10^{11}$ have been found, which translate into ballistic carrier transport in the micrometer range.[8] No other known material has yet been able to exhibit electron- or hole mobilities comparable to those of single- or few-layer graphene. SCAs currently represent one of the most promising material families with enormous potential for high-performance applications in the fields of nanoelectronics, optoelectonics, hydrogen storage, sensors, and reinforcements of polymers based on their unprecedented electronic, optical, mechanical, and chemical properties. At the same time they are ideal targets for the investigation of fundamental chemical and physical questions such as shape- and charge-dependent binding and release of molecules, charge transport in confined spaces, and superior sensing of supramolecular interactions down to the single molecule regime.

Tapping these exciting possibilities, however, still requires overcoming a number of significant obstacles such as high-yield production methods, sorting and separation, controlled doping with heteroatoms, development of hierarchically ordered architectures, layer (single and multiple) formation, processing, and solubilization. Chemical functionalization of synthetic carbon allotropes (SCAs) is certainly a key for the systematic development of SCA-technology, since covalent and noncovalent derivatization allows for (a) increasing, tuning, and adjusting the solubility, dispersibility, and processability both on aqueous and organic media and (b) modifying and tailoring electronic, optical, and mechanical properties, (c) separation and isolation of specific types (e.g., tube chiralities and helicities), and (d) construction of ordered two-and three-dimensional superstructures. Moreover, the investigation of the chemical behavior and reactivity of SCAs itself represent an exciting research subject on its own right. In principle, the physical and chemical properties of fullerenes, carbon nanotubes (CNTs), and graphene are related to each other, although their levels of development vary considerably. Whereas the chemistry of fullerenes has already achieved a rather mature state and numerous derivatives have been synthesized and characterized[9] in detail, functionalization of graphene is still in its infancy.[10] Carbon nanotube chemistry keeps an intermediate position.[11] Compared to the various flavors of carbon nanotubes (broad variation of helicities, single walled, multiwalled) graphene is a much more uniform material. This will facilitate the development of its chemistry considerably. In contrast to the fullerenes and carbon nanotubes, which exhibit exo and endo faces, covalent attacks to graphene are possible from both sides of the plane. Appealing synthetic targets are inter alia graphane and its alkyl-, aryl-, and fluoro derivatives which represent the first prototypes of two-dimensional-polymers, dye-functionalized graphene for the photoinduced H_2-generation, and polymer-functionalized graphene as stable building block for the construction of electroactive composite materials. Many protocols that have been efficiently used for the functionalization of fullerenes and carbon nanotubes are expected to be transferred successfully for the chemical derivatization of this novel two-dimensional SCA.

Our laboratory has a long experience in carbon allotrope chemistry. In the early 1990s, we started with the investigations of basic principles for the functionalization of fullerenes and later on with that of carbon nanotubes. Among our most important achievements are control over the regiochemistry of multiple addition reactions to fullerenes,[12] the shape-dependent difference of endohedral and exohedral functionalization, the $2(n + 1)^2$-rule for the description of spherical aromaticity of fullerenes,[13] the introduction of water solubility into these carbon rich systems,[14,15] and the first *p*-type doping of carbon nanotubes.[16] A large variety of fullerene and nanotube derivatives with tailor-made properties have been prepared and characterized such as (a) donor−acceptor hybrids suitable to undergo photoinduced energy- and electron transfer,[17] (b) synthetic mimics for globular hemeproteins,[18] (c) dendrizymes,[19] (d) heterofullerenes,[20] (e) the largest polyelectrolytes with completely defined and monodisperse structures,[21] (f) nanotube based carriers for gene delivery,[22] (g) giant bis-fullerene dipoles,[23] (h) the first example of fullerene amphiphiles that self-assemble in fully shape persistent micelles,[24] whose structure could be determined with molecular precision, and (i) water-soluble fullerene derivatives that act as very potent superoxide dismutase models[25] in the field of biomedical chemistry.

With this knowledge at hand, we started in 2009 with the investigation of the wet chemistry of graphene. In this Account we will summarize our first results on graphene functionalization, categorized in noncovalent and covalent functionalization, respectively.

Noncovalent Functionalization

On the basis of our experience in the π-surfactant mediated dispersion of carbon nanotubes in water,[26−31] we first targeted the idea of exfoliating graphite to generate individual graphene sheets stabilized by noncovalent interactions

with suitable surfactants that contained an extended conjugated π-system.[15] An example is the perylene derivative **1**, representing a member of the first family of very water-soluble rylenes, that we have recently made synthetically available.[32] These molecules exhibit superior performance in terms of solubilization and individualization of carbon nanotubes, driven by a combination of π/π-stacking and hydrophobic interactions.[14] The appealing opportunity of this idea was that not only the supramolecular interactions of graphene with rylenes could be studied but also wet chemical graphene production in bulk quantities could be accomplished. At that time the typical methods to access graphene still were mechanical scotch tape exfoliation of graphite[3] or silicon evaporation from SiC[33] that led and still lead to very limited amounts of material.

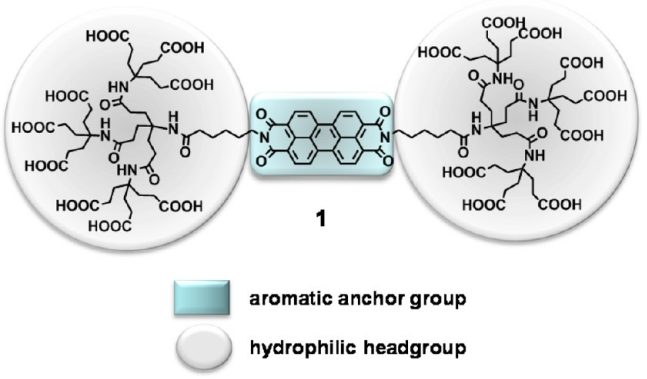

In the beginning, we were rather unsure whether this approach would be successful because in order to generate individualized graphene sheets out of graphite, the most obvious challenge is to overcome the huge amount of energy which is stored in the π/π-stacking interactions between the extended graphene sheets. The cohesive energy gained by stacking graphene sheets onto each other was experimentally determined to be as high as 61 meV/C-atom.[34] On the other hand, the mechanical exfoliation method used to access graphene clearly showed that the intermolecular π/π-stacking interactions between the basal planes can be overcome by pronounced interactions with substrates. With suitable postprocessing, the extrinsic corrugation of the substrate can be further utilized to improve the yield of mechanically exfoliated layers.[35] The group of Coleman has shown that in principle also wet chemical dispersion of graphite or few layer graphene (FLG) driven by multiple noncovalent interactions with suitable solvent molecules such as *N*-methylpyrrolidone (NMP) is possible.[36] Encouraged by these findings and our own results on carbon nanotube exfoliation,[26−31] we expected that the combination of π/π-stacking and hydrophobic effect driven dispersion of graphite should be a feasible approach. However, it was also clear that next to the efficient exfoliation itself, the unambiguous characterization and analysis of the noncovalent graphene functionalization would be a very challenging task.

Investigations on a monodisperse model system for graphene with a defined structure, however, could provide valuable insights and facilitate the interpretation of experimental results. For this purpose we chose hexa-peri-benzocoronene (HBC), which exhibits precisely defined optical absorption and emission features while resembling many of the aggregation phenomena of graphite.[37] For example, HBC forms π-stacks in the crystal and is characterized by very low solubility in common organic solvents.[38]

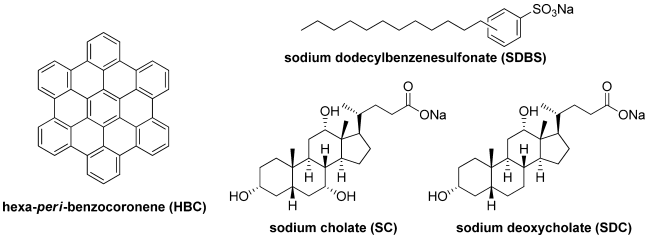

Thus, it could be anticipated that conditions which yield HBC monomers in water would also result in appreciable yields of graphene monolayers. First investigations based on commercially available surfactants such as sodium dodecylbenzenesulfonate (SDBS), sodium cholate (SC), and sodium deoxycholate (SDC) were carried out in our laboratories and indeed revealed significant differences in material uptake and individualization efficiencies. While the highest overall material uptake could be observed in amphiphilic SDBS dispersions, the use of SDC leads by far to the highest degrees of individualization. Individualized HBC molecules were easily identified by their characteristic emission pattern[39] and quantified by fluorescence lifetime analysis.

These results gave us confidence that aromatic surfactants such as the perylene derivative **1** will yield stable graphene dispersions. When we ultrasonicated graphite in the typical red-colored aqueous solutions of **1**, we observed the formation of black inks. Since after sedimentation the homogeneous solutions remained dark, we concluded that our surfactant based strategy for graphene formation was successful. We then prepared stock solutions of few-layer (FLG) and single-layer graphene (SLG) by the stepwise addition and ultrasonication of **1** to a dispersion of pristine graphite in buffered water at pH 7. The corresponding absorption spectra confirmed the proposed exfoliation of graphene. Except for a broad peak between 250 and 300 nm and the characteristic absorption patterns of **1**, the

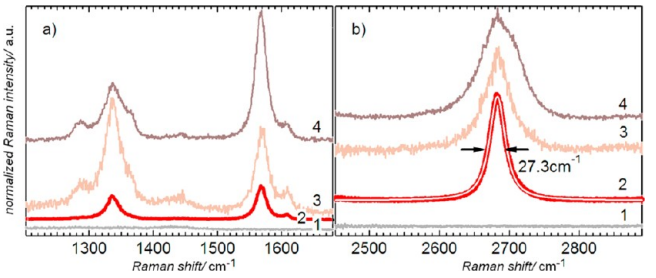

FIGURE 1. Raman spectra of the D and G peaks (a) and the 2D peak (b) taken at the positions indicated in Figure 2. The analysis of the line recorded at position 2 shows a single symmetric component with fwhm = 27.3 cm^{-1} characteristic for SLG. The symmetrical fit function is superimposed on the experimental data in spectrum 2. Reproduced with permission from ref 15. Copyright 2009 Wiley-VCH.

spectra were featureless especially in the visible and nIR-regime. For a more detailed characterization of the dispersed material, we spin-casted the supernatant solution onto a silicon wafer coated with a 300 nm thick layer of SiO_2. This enabled us to analyze the deposited material by optical microscopy through interference from rays reflected from the Si/SiO_2 interface and the graphene/SiO_2 interface.[40,41] The images revealed objects with lateral dimensions of hundreds of nanometers and an optical contrast in agreement with very thin deposits as expected for FLG and SLG. Similar conclusions could be deduced from AFM-studies. For an unequivocal proof of the presence of solution processed single layer graphene on the solid support, we carried out high spatial resolution scanning Raman microscopy (Figure 1). Especially the shape and the width of the so-called 2D peak, which is recorded at around 2700 cm^{-1} and corresponds to the excitation of two momentum conserving phonons close to the K-point in the Brillouin zone, are very indicative of the presence or absence of a single layer graphene.[42]

We were able to categorize the spectra into SLG, FLG, and multilayer graphene (MLG) and visualize the distribution of the respective species. Even after spin-casting and drying, which is certainly accompanied by some reaggregation of graphene, a substantial amount of SLG deposits could be identified (Figure 2).

Next to the wet chemical graphene formation itself, we were interested in a detailed insight of the nature of the noncovalent interaction with perylenes, in particular the electronic communication between the corresponding π-systems.[43] For this purpose, we used turbostratic graphite as the starting material. In this type of graphite, the arrangement between the basal planes is disordered and as a consequence the interlayer coupling is typically less pronounced than in natural graphite, which is characterized by a high degree of crystallinity. The turbostratic nature of the graphite allowed one to prepare sufficiently stable dispersions by ultrasound mediated exfoliation of the material in NMP. After centrifugation, stable homogeneous solutions of SLG and FLG were obtained. For the investigation of the noncovalent interaction with perylenes, we added a NMP solution of the amphiphilic derivative **2**.

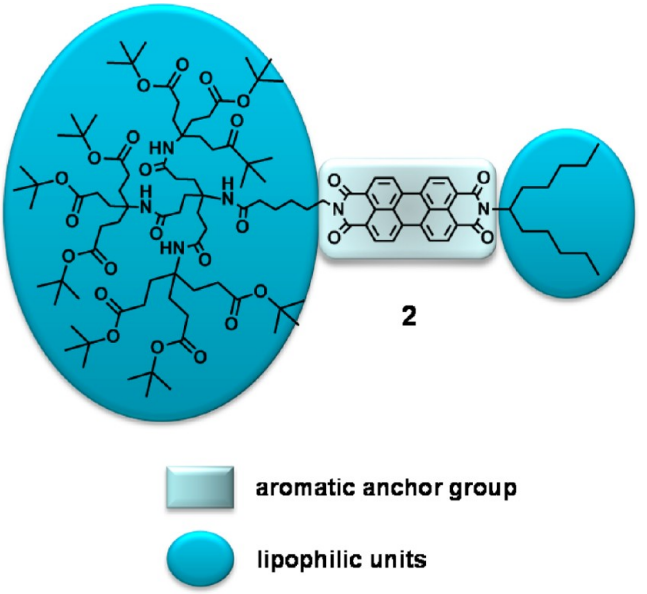

Although perylenes exhibit a very strong fluorescence, which is usually preventing their investigation by Raman spectroscopy, we were able to record a resonantly enhanced Raman spectrum of the graphene/perylene-**2** deposit on Si/SiO_2 comprising the features of both graphene and perylene, when excited at 532 nm (Figure 3). The possibility to acquire the Raman spectrum of **2** is owed to the fact that the pronounced fluorescence of **2** is completely quenched in the presence of graphene. When excited at 633 nm, which is beyond the region of perylene absorptions, only graphene features can be observed in the Raman spectra (Figure 3).

We were also able to visualize the graphene induced quenching of the perylene fluorescence by fluorescence microscopy on the deposits (Figure 4).

For a more detailed investigation of the electronic communication and the noncovalent binding of graphene and **2** in homogeneous solution, we carried out a series of titration experiments. The plots of the fluorescence intensities of the perylene emission as a function of the absorption revealed fluorescence quenching (Figure 5) as the emission of **2** is always significantly smaller in the presence of graphene. The slopes of the fitted linear dependencies are proportional to the corresponding fluorescence quantum yields. In the

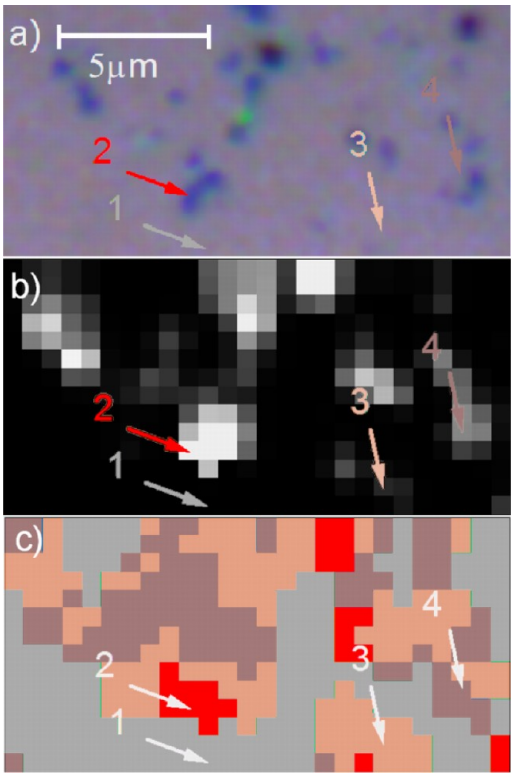

FIGURE 2. (a) Optical microscopy image of graphene deposited on a Si/SiO_2 substrate with a 300 nm thick oxide layer. The arrows denote the areas where the Raman spectra shown in Figure 1 were taken: (b) Raman amplitude of the 2D peak, (c) map of the fwhm (2D peak). Red areas: 25−39 cm^{-1} (SLG); ocher areas, 39−65 cm^{-1} (FLG); brown areas, > 65 cm^{-1} (MLG). Reproduced with permission from ref 15. Copyright 2009 Wiley-VCH.

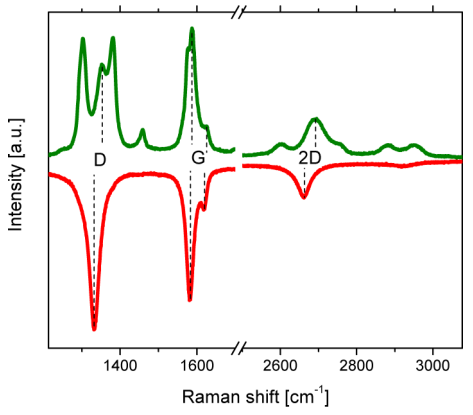

FIGURE 3. Raman spectra of the dispersion of turbostratic graphite with perylenes-**2** in NMP. At 532 nm excitation (green spectrum), both characteristic SLG and MLG peaks (marked as D-, G-, and 2D-bands) and peaks that originate from **2** are observed. It is possible to record the Raman spectrum of **2** due to fluorescence quenching by graphene. Reproduced with permission from ref 43. Copyright 2010 Wiley-VCH.

presence of graphene, the fluorescence quantum yield of **2** is reduced to 65% with respect to the stock perylene solution.

In order to carry out a structural characterization of graphene/perylene-**2** composite, we carried out high-resolution transmission electron microscopy (HRTEM) using a Titan^3 microscope equipped with an image aberration corrector. Single crystalline "terraces" decorated with amorphous material could be observed (Figure 6). The fast Fourier transformed image shown in the inset of Figure 6 reveals the expected 6-fold carbon lattice symmetry. After Fourier-filtering with the crystalline reflections, the amorphous contrast could be removed and the pattern closely resembled the projected atomic structure.

Covalent Functionalization

In contrast to the wet chemical exfoliation of graphene from graphite, which used noncovalently binding surfactants or solvent molecules, covalent addition of reactive molecules to graphene would lead to the introduction of sp^3-defects or even rupture of the carbon framework. As a consequence, the intrinsic electronic properties will be altered considerably. On the other hand, covalent binding of addends provides the opportunity to permanently stabilize graphene sheets. This offers the potential to considerably improve the solubility and processability. A subsequent thermal treatment of covalently functionalized graphene is expected to restore the intrinsic electronic and mechanical properties by retro-functionalization.[44,45] The latter course would only apply to those cases where only sp^3-defects and no holes within the carbon framework are introduced. Once larger and hence more irremediable defects such as holes are formed, for example, by harsh oxidative treatments (Hummer's GO),[46] such treatment becomes significantly more demanding. It is therefore a challenge to develop a mild covalent graphene chemistry that introduces solely sp^3-defects. Further advantages of covalent graphene chemistry are to tune electronic properties like a band gap systematically and combine graphene properties with those of other compound classes that bear specific functions. Moreover, the investigation of the reaction mechanisms and the intrinsic chemical behavior of graphene per se is of utmost general interest. The ultimate product of graphene addition chemistry would be graphane, where every C-atom carries a hydrogen addend. Graphane, where every six-membered ring has a chair conformation, would be an unstrained and hence very stable system and could be formed by the alternating 1,2-binding of H-atoms from above and below the basal plane. Because of their curved and closed cage structure, which is effectively preventing the entry and endohedral binding of H-atoms, the alternating endo/exo

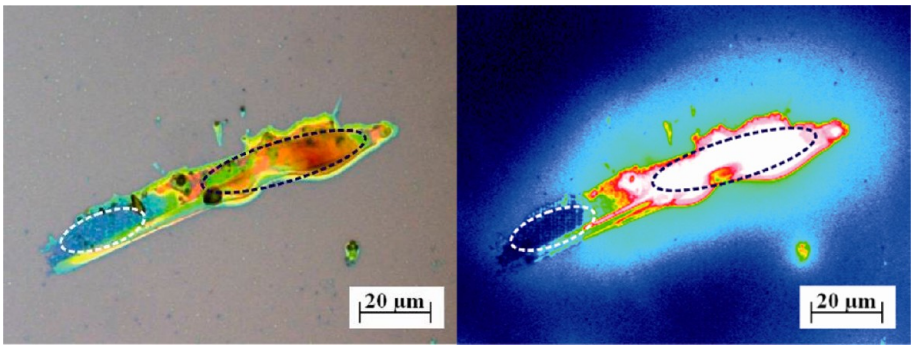

FIGURE 4. Micrographs of graphene-perylene dispersion. (Left) White light illumination, blue contrast corresponds to graphene and finely dispersed graphite particles (marked with white oval). (Right) Falsecolored fluorescence image (green light excitation up to 545 nm, emission was collected starting with 605 nm). Emission is observed for the unbound perylene and is quenched when interaction with graphene takes place (marked with a white oval). Reproduced with permission from ref 43. Copyright 2010 Wiley-VCH.

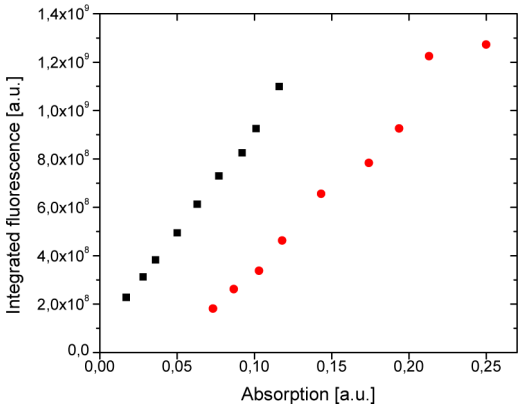

FIGURE 5. Integrated fluorescence vs absorption for perylene-**2** NMP solution "titrated" with pure NMP (black) and perylene-**2** NMP solution titrated with graphene dispersion in NMP (red). Excitation performed and absorption plotted at 490 nm. The slopes for the linear fits of the two data sets are proportional to the relative quantum yields for the two above-mentioned systems. The ratio of the slopes gives a value of ~65% due to fluorescence quenching. Reproduced with permission from ref 43. Copyright 2010 Wiley-VCH.

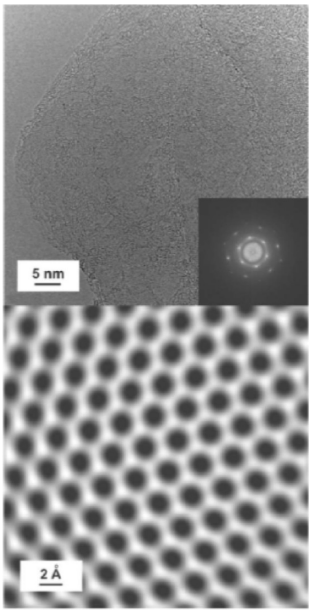

FIGURE 6. (Top) HRTEM image (300 kV) of a graphitic flake of a graphene/perylene-**2** sample. (Inset) Fast Fourier Transform (FFT) reveals the hexagonal symmetry. (Bottom) Magnified view of the HRTEM image after Fourier-filtering with the crystalline reflections. Reproduced with permission from ref 43. Copyright 2010 Wiley-VCH.

addition pattern is not observed for fullerenes and carbon nanotubes. Early examples of covalent graphene chemistry are additions of azomethine ylides[47] and benzynes.[48] Also edge selective functionalizations that rely on Friedl-Crafts like acylation have been reported so far.[49]

On the basis of our experience with carbon nanotube chemistry,[50−55] we followed a new and highly efficient approach for covalent graphene functionalization. The idea was to reduce graphite, for example, by alkali metals in liquid ammonia, which on the one hand would facilitate exfoliation due to electrostatic repulsion and on the other hand would activate the graphene sheet for subsequent reactions, for example, with electrophilic addends. Although graphite is chemically rather inert, it has been known for a long time that it can undergo intercalation reactions with small inorganic molecules or alkaline metals.[10,56] In the latter graphite intercalation compounds (GICs), positively charged metal cations are located in between the negatively charged graphene sheets. Therefore, the interlayer distance is increased to 5.40 Å in the first stage K-GIC, and the direct $\pi-\pi$-interaction between two adjacent layers is decreased while an electrostatic host/guest attraction is introduced.[56] GICs like the golden to bronze colored KC_8 are known to be efficient reducing agents. After the treatment of KC_8 with polar aprotic solvents under inert gas conditions, evidence for dissolved negatively charged graphene was found.[57,58] We expected that such a balanced combination of intercalation

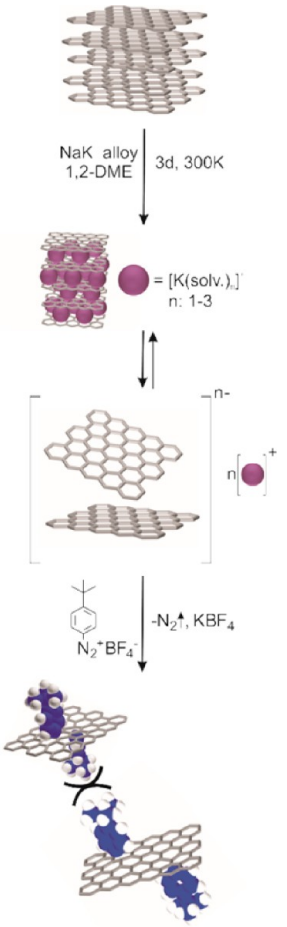

FIGURE 7. Representation of the intercalation and exfoliation of graphite with subsequent functionalization of intermediately generated reduced graphene that yield 4-*tert*-butylphenyl functionalized graphene. Reprinted by permission from Macmillan Publishers Ltd: *Nature Chemistry* Englert, J. M.; Dotzer, C.; Yang, G.; Schmid, M.; Papp, C.; Gottfried, J. M.; Steinrück, H.-P.; Spiecker, E.; Hauke, F.; Hirsch, A. Covalent bulk functionalization of graphene. *Nat. Chem.* **2011**, *3*, 279−286, copyright 2011.

combined with Coulomb driven repulsion could in principle open the door for an efficient exfoliation and wet chemical functionalization of the electronically activated graphene sheets via recombination with reactive addends.[59] First, we investigated the treatment of reduced graphite with aryl diazonium salts (Figure 7). The corresponding reaction is well-known for carbon nanotubes and yields arylated and exfoliated derivatives after the elimination of N_2.

In the case of the wet chemical graphene functionalization, we have prepared the reduced graphene by the treatment with sodium/potassium alloys in 1,2-dimethoxyethane (DME) as an inert and electride/alkalide stabilizing solvent. To work in DME in contrast to the more commonly applied liquid ammonia (classical Birch conditions) offers the

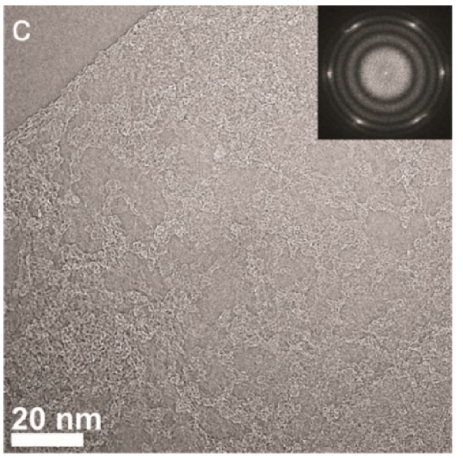

FIGURE 8. HRTEM micrographs of functionalized graphene derivatives. High functionalization density leads to the formation of amorphous regions among crystalline domains, as is visible in the HRTEM image and also in the fast Fourier transformation FFT pattern. Adapted with permission from Macmillan Publishers Ltd: *Nature Chemistry* Englert, J. M.; Dotzer, C.; Yang, G.; Schmid, M.; Papp, C.; Gottfried, J. M.; Steinrück, H.-P.; Spiecker, E.; Hauke, F.; Hirsch, A. Covalent bulk functionalization of graphene. *Nat. Chem.* **2011**, *3*, 279−286, copyright 2011.

opportunity to work at room temperature and also allows the use of a broad variety of diazonium compounds in solution as DME does not decompose the labile diazonium moiety. As expected, the addition of the diazonium salt to the dispersion of reduced and exfoliated graphene sheets was accompanied by vigorous nitrogen evolution. After the reaction was completed, we have isolated the functionalized graphene by means of spin-casting, filtration, or dip-coating for spectroscopic and microscopic characterization. Interestingly, structural analysis by HRTEM showed the formation of domains of arylated regions rather than homogeneous addition to the flake (Figure 8). Similar regioselectivities have already been observed in fullerene[60] and carbon nanotube chemistry,[61] and future theoretical studies are required for understanding this behavior completely.

The introduction of heteroatom containing groups such as sulfonic acid substituents at the aryl addends allowed for additional characterization by elemental and chemical analysis through energy-dispersive X-ray spectroscopy (EDX) and X-ray photoelectron spectroscopy (XPS). Particularly powerful for the characterization of the reactions products was Raman microscopy. The addition of an aryl addend, which is accompanied by the introduction of a sp^3-defect, becomes apparent by an increase of the D-peak (Figure 9a). At the same time, the 2D-peak sharpens and becomes more symmetrical, finally reaching a Lorenzian shape, which is characteristic for decoupled graphene monolayers.[42] Spatially resolved Raman mappings greatly facilitated the

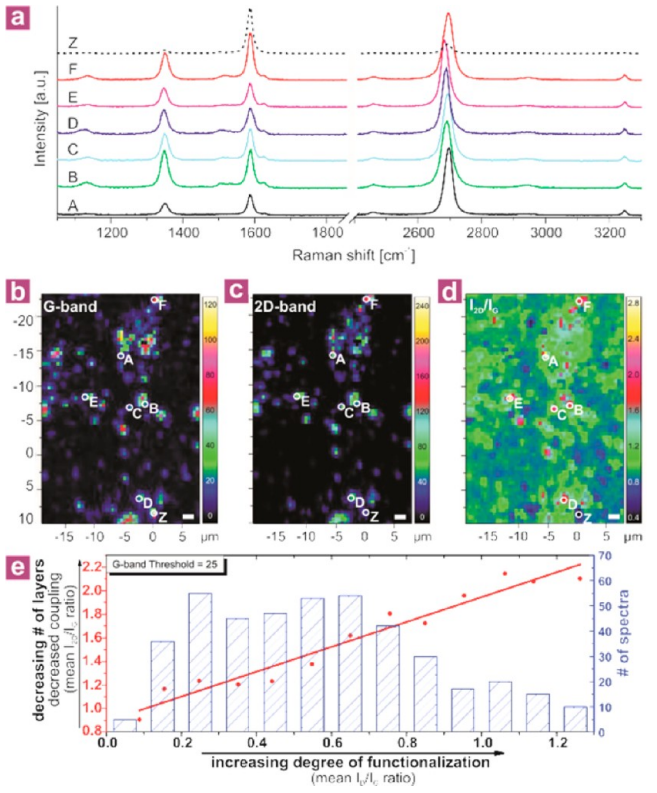

FIGURE 9. (a) Raman spectra recorded from the corresponding spots indicated in mappings b, c and d. (b) Spatial G-band intensity distribution. (c) Spatial 2D-band intensity distribution. (d) Spatial distribution of the I_{2D}/I_G ratio. (e) Linear correlation between the defect density and the I_{2D}/I_G ratio as a suitable measure of the monolayer character. The histogram represents the number of spectra found for each I_D/I_G interval.

quantitative analysis of the bulk material in terms of the distribution of the degrees of functionalization and individualization (Figure 9b).

Annealing of the material at 1000 °C under inert gas atmosphere allowed for the complete regeneration of the hexagonal carbon network contrary to graphene oxide, where a complete restoration is more difficult. This complete reversibility is combined with the possibility of varying both the nature of the addend and the degree of functionalization to a large extent. Hence, these new graphene modification protocols provide access to a broad variety of functional and processable graphenes with tailored properties. Indeed, we have shown recently that also other reagents like alkyliodides[62] and CO_2 can be applied successfully for the wet chemical trapping of the reduced graphene sheets.

Conclusion and Oulook

Although the development of graphene chemistry has just begun to emerge, a number of promising functionalization concepts have already been introduced. On the basis of our experience with fullerenes and carbon nanotubes, we have recently elaborated a series of covalent and noncovalent approaches for the generation of new graphene derivatives. As a consequence, the door for combining the unprecedented graphene properties with those of other compound classes has been opened. One can expect that graphene based high-performance materials will find interesting applications, for example, in the field of nano- and transparent electronics. Of course a lot of fundamental research is still required to approach this attractive prospect. In this regard, with increasing knowledge of inherent graphene reactivity principles, further improvement of characterization methods as well as the ability to selectively synthesize graphene derivatives with a highly specific functionality will be of central future importance.

We thank the Deutsche Forschungsgemeinschaft in particular the SFB 953 "Synthetic Carbon Allotropes" and the European Research Council (ERC); Grant 24662—GRAPHENOCHEM for financial support.

BIOGRAPHICAL INFORMATION

Andreas Hirsch was born in Esslingen, Germany, in 1960 and received his doctoral degree in 1990 from the University of Tübingen. Following postdoctoral studies at the Institute for Polymers and Organic Solids at UCSB from 1990 to 1991, he was a research associate at the Institute of Organic Chemistry at the University of Tübingen. After his habilitation in 1994, he joined the faculty of the University of Karlsruhe as professor of organic chemistry (March 1995). Since October 1995, he is professor of organic chemistry at the University of Erlangen-Nürnberg.

Jan M. Englert was born in Bamberg, Germany, in 1983 and received his BSc degree in molecular science from the University of Erlangen-Nürnberg in 2007. He finished his MSc in Molecular Nanoscience in 2009. He is currently working in the group of Andreas Hirsch on his Ph.D. thesis devoted to the chemical functionalization of graphene.

Frank Hauke was born in Erlangen, Germany, in 1972 and received his Ph.D. in 2003 from the University of Erlangen-Nuremberg. After a 2 year postdoctoral stay from 2004—2006 at the Scripps Research Institute, La Jolla, CA, he commenced his research activities at the Institute of Advanced Materials and Processes, Fürth (University Erlangen-Nuremberg) as chief executive and group leader in the field of functional carbon allotropes.

FOOTNOTES

*To whom correspondence should be addressed. E-mail: andreas.hirsch@chemie.uni-erlangen.de.

The authors declare no competing financial interest.

REFERENCES

1 Kroto, H. W.; Heath, J. R.; O'Brien, S. C.; Curl, R. F.; Smalley, R. E. C_{60}: Buckminsterfullerene. *Nature* **1985**, *318*, 162–163.

2 Iijima, S. Helical microtubules of graphitic carbon. *Nature* **1991**, *354*, 56–58.

3 Novoselov, K. S.; Geim, A. K.; Morozov, S. V.; Jiang, D.; Zhang, Y.; Dubonos, S. V.; Grigorieva, I. V.; Firsov, A. A. Electric Field Effect in Atomically Thin Carbon Films. *Science* **2004**, *306*, 666–669.

4 Hirsch, A. The era of carbon allotropes. *Nat. Mater.* **2010**, *9*, 868–871.

5 Malko, D.; Neiss, C.; Viñes, F.; Görling, A. Competition for Graphene: Graphynes with Direction-Dependent Dirac Cones. *Phys. Rev. Lett.* **2012**, *108*, 086804.

6 Allen, M. J.; Tung, V. C.; Kaner, R. B. Honeycomb Carbon: A Review of Graphene. *Chem. Rev.* **2009**, *110*, 132–145.

7 Chen, J.-H.; Jang, C.; Xiao, S.; Ishigami, M.; Fuhrer, M. S. Intrinsic and extrinsic performance limits of graphene devices on SiO_2. *Nat. Nanotechnol.* **2008**, *3*, 206–209.

8 Du, X.; Skachko, I.; Barker, A.; Andrei, E. Y. Approaching ballistic transport in suspended graphene. *Nat. Nanotechnol.* **2008**, *3*, 491–495.

9 Hirsch, A.; Brettreich, M. *Fullerenes - Chemistry and Reactions*; Wiley-VCH: Weinheim, Germany, 2005.

10 Malig, J.; Englert, J. M.; Hirsch, A.; Guldi, D. M. Wet chemistry of graphene. *Electrochem. Soc. Interface* **2011**, *20*, 53–56.

11 Hauke, F.; Hirsch, A. In *Carbon Nanotubes and Related Structures*; Guldi, D. M., Martín, N., Eds.; Wiley-VCH: Weinheim, Germany, 2010; pp 135−198.

12 Hirsch, A.; Lamparth, I.; Groesser, T.; Karfunkel, H. R. Regiochemistry of Multiple Additions to the Fullerene Core: Synthesis of a T_h-Symmetric Hexakis adduct of C_{60} with Bis-(ethoxycarbonyl)methylene. *J. Am. Chem. Soc.* **1994**, *116*, 9385–9386.

13 Chen, Z.; Jiao, H.; Hirsch, A.; Schleyer, P. v. R. Spherical homoaromaticity. *Angew. Chem., Int. Ed.* **2002**, *41*, 4309–4312.

14 Backes, C.; Schmidt, C. D.; Hauke, F.; Böttcher, C.; Hirsch, A. High population of individualized SWCNTs through the adsorption of water-soluble perylenes. *J. Am. Chem. Soc.* **2009**, *131*, 2172–2184.

15 Englert, J. M.; Roehrl, J.; Schmidt, C. D.; Graupner, R.; Hundhausen, M.; Hauke, F.; Hirsch, A. Soluble Graphene: Generation of Aqueous Graphene Solutions Aided by a Perylenebisimide-Based Bolaamphiphile. *Adv. Mater.* **2009**, *21*, 4265–4269.

16 Ehli, C.; Oelsner, C.; Guldi, D. M.; Mateo-Alonso, A.; Prato, M.; Schmidt, C.; Backes, C.; Hauke, F.; Hirsch, A. Manipulating single-wall carbon nanotubes by chemical doping and charge transfer with perylene dyes. *Nat. Chem.* **2009**, *1*, 243–249.

17 Guldi, D. M.; Luo, C.; Da Ros, T.; Prato, M.; Dietel, E.; Hirsch, A. Photoinduced electron transfer in multicomponent arrays of a π-stacked fullerene porphyrin dyad and diazabicyclooctane or a fulleropyrrolidine ligand. *Chem. Commun.* **2000**, 375–376.

18 Camps, X.; Dietel, E.; Hirsch, A.; Pyo, S.; Echegoyen, L.; Hackbarth, S.; Röder, B. Globular Dendrimers Involving a C_{60} Core and a Tetraphenyl Porphyrin Function. *Chem.—Eur. J.* **1999**, *5*, 2362–2373.

19 Maurer, K.; Grimm, B.; Wessendorf, F.; Hartnagel, K.; Guldi, D. M.; Hirsch, A. Self-Assembling Depsipeptide Dendrimers and Dendritic Fullerenes with New cis- and trans-Symmetric Hamilton Receptor Functionalized Zn−Porphyrins: Synthesis, Photophysical Properties and Cooperativity Phenomena. *Eur. J. Org. Chem.* **2010**, *2010*, 5010–5029.

20 Hirsch, A.; Nuber, B. Nitrogen Heterofullerenes. *Acc. Chem. Res.* **1999**, *32*, 795–804.

21 Witte, P.; Hörmann, F.; Hirsch, A. Large Di- and Heptafullerene Polyelectrolytes Composed of C60 Building Blocks Having a Highly Symmetrical Hexakisaddition Pattern. *Chem.—Eur. J.* **2009**, *15*, 7423–7433.

22 Krajcik, R.; Jung, A.; Hirsch, A.; Neuhuber, W.; Zolk, O. Functionalization of carbon nanotubes enables non-covalent binding and intracellular delivery of small interfering RNA for efficient knock-down of genes. *Biochem. Biophys. Res. Commun.* **2008**, *369*, 595–602.

23 Hauke, F.; Herranz, M. A.; Echegoyen, L.; Guldi, D.; Hirsch, A.; Atalick, S. The first fullerene-heterofullerene dyad. *Chem. Commun.* **2004**, 600–601.

24 Kellermann, M.; Bauer, W.; Hirsch, A.; Schade, B.; Ludwig, K.; Boettcher, C. The first account of a structurally persistent micelle. *Angew. Chem., Int. Ed.* **2004**, *43*, 2959–2962.

25 Liu, G.-F.; Filipović, M.; Ivanović-Burmazović, I.; Beuerle, F.; Witte, P.; Hirsch, A. High Catalytic Activity of Dendritic C_{60} Monoadducts in Metal-Free Superoxide Dismutation. *Angew. Chem., Int. Ed.* **2008**, *47*, 3991–3994.

26 Backes, C.; Hauke, F.; Schmidt, C. D.; Hirsch, A. Fractioning HiPco and CoMoCAT SWCNTs via density gradient ultracentrifugation by the aid of a novel perylene bisimide derivative surfactant. *Chem. Commun.* **2009**, 2643–2645.

27 Backes, C.; Schmidt Cordula, D.; Rosenlehner, K.; Hauke, F.; Coleman Jonathan, N.; Hirsch, A. Nanotube surfactant design: the versatility of water-soluble perylene bisimides. *Adv. Mater.* **2010**, *22*, 788–802.

28 Backes, C.; Hauke, F.; Hirsch, A. The Potential of Perylene Bisimide Derivatives for the Solubilization of Carbon Nanotubes and Graphene. *Adv. Mater.* **2011**, *23*, 2588–2601.

29 Backes, C.; Mundloch, U.; Ebel, A.; Hauke, F.; Hirsch, A. Dispersion of HiPco and CoMoCAT Single-Walled Nanotubes (SWNTs) by Water Soluble Pyrene Derivatives-Depletion of Small Diameter SWNTs. *Chem.—Eur. J.* **2010**, *16*, 3314–3317.

30 Backes, C.; Hirsch, A. In *Chemistry of Nanocarbons*; Akasaka, T., Wudl, F., Nagase, S., Eds.; John Wiley & Sons Ltd.: Chichester, U.K., 2010; pp 1−48.

31 Backes, C.; Mundloch, U.; Schmidt, C. D.; Coleman, J. N.; Wohlleben, W.; Hauke, F.; Hirsch, A. Enhanced Adsorption Affinity of Anionic Perylene-Based Surfactants towards Smaller-Diameter SWCNTs. *Chem.—Eur. J.* **2010**, *16*, 13185–13192.

32 Schmidt, C. D.; Böttcher, C.; Hirsch, A. Synthesis and Aggregation Properties of Water-Soluble Newkome-Dendronized Perylenetetracarboxdiimides. *Eur. J. Org. Chem.* **2007**, 5497–5505.

33 Berger, C.; Song, Z.; Li, X.; Wu, X.; Brown, N.; Naud, C.; Mayou, D.; Li, T.; Hass, J.; Marchenkov, A. N.; Conrad, E. H.; First, P. N.; de Heer, W. A. Electronic confinement and coherence in patterned epitaxial graphene. *Science* **2006**, *312*, 1191–1196.

34 Zacharia, R.; Ulbricht, H.; Hertel, T. Interlayer cohesive energy of graphite from thermal desorption of polyaromatic hydrocarbons. *Phys. Rev. B* **2004**, *69*, 1–7.

35 Pang, S.; Englert, J. M.; Tsao, H. N.; Hernandez, Y.; Hirsch, A.; Feng, X.; Müllen, K. Extrinsic corrugation-assisted mechanical exfoliation of monolayer graphene. *Adv. Mater.* **2010**, *22*, 5374–5374.

36 Hernandez, Y.; Nicolosi, V.; Lotya, M.; Blighe, F. M.; Sun, Z.; De, S.; McGovern, I. T.; Holland, B.; Byrne, M.; Gun'Ko, Y. K.; Boland, J. J.; Niraj, P.; Duesberg, G.; Krishnamurthy, S.; Goodhue, R.; Hutchison, J.; Scardaci, V.; Ferrari, A. C.; Coleman, J. N. High-yield production of graphene by liquid-phase exfoliation of graphite. *Nat. Nanotechnol.* **2008**, *3*, 563–568.

37 Englert, J. M.; Hauke, F.; Feng, X.; Muellen, K.; Hirsch, A. Exfoliation of hexa-peri-hexabenzocoronene in water. *Chem. Commun.* **2010**, *46*, 9194–9196.

38 Watson, M. D.; Fechtenkötter, a.; Müllen, K. Big is beautiful—"aromaticity" revisited from the viewpoint of macromolecular and supramolecular benzene chemistry. *Chem. Rev.* **2001**, *101*, 1267–1300.

39 Kastler, M.; Pisula, W.; Wasserfallen, D.; Pakula, T.; Müllen, K. Influence of alkyl substituents on the solution- and surface-organization of hexa-peri-hexabenzocoronenes. *J. Am. Chem. Soc.* **2005**, *127*, 4286–4296.

40 Blake, P.; Hill, E. W.; Castro Neto, a. H.; Novoselov, K. S.; Jiang, D.; Yang, R.; Booth, T. J.; Geim, a. K. Making graphene visible. *Appl. Phys. Lett.* **2007**, *91*, 063124.

41 Backes, C.; Englert, J. M.; Bernhard, N.; Hauke, F.; Hirsch, A. Optical Visualization of Carbon Nanotubes - a Unifying Linkage Between Microscopic and Spectroscopic Characterization Techniques. *Small* **2010**, *6*, 1968–1973.

42 Ferrari, A. C.; Meyer, J.; Scardaci, V.; Casiraghi, C.; Lazzeri, M.; Mauri, F.; Piscanec, S.; Jiang, D.; Novoselov, K.; Roth, S.; Geim, a. Raman Spectrum of Graphene and Graphene Layers. *Phys. Rev. Lett.* **2006**, *97*, 1–4.

43 Kozhemyakina, N. V.; Englert, J. M.; Yang, G.; Spiecker, E.; Schmidt, C. D.; Hauke, F.; Hirsch, A. Non-Covalent Chemistry of Graphene: Electronic Communication with Dendronized Perylene Bisimides. *Adv. Mater.* **2010**, *22*, 5483–5487.

44 El-Kady, M. F.; Strong, V.; Dubin, S.; Kaner, R. B. Laser Scribing of High-Performance and Flexible Graphene-Based Electrochemical Capacitors. *Science* **2012**, *335*, 1326–1330.

45 Strong, V.; Dubin, S.; El-Kady, M. F.; Lech, A.; Wang, Y.; Weiller, B. H.; Kaner, R. B. Patterning and Electronic Tuning of Laser Scribed Graphene for Flexible All-Carbon Devices. *ACS Nano* **2012**, *6*, 1395–1403.

46 Hummers, W. S., Jr; Offeman, R. E. Preparation of graphitic oxide. *J. Am. Chem. Soc.* **1958**, *80*, 1339–1339.

47 Quintana, M.; Spyrou, K.; Grzelczak, M.; Browne, W. R.; Rudolf, P.; Prato, M. Functionalization of graphene via 1,3-dipolar cycloaddition. *ACS Nano* **2010**, *4*, 3527–3533.

48 Zhong, X.; Jin, J.; Li, S.; Niu, Z.; Hu, W.; Li, R.; Ma, J. Aryne cycloaddition: highly efficient chemical modification of graphene. *Chem. Commun.* **2010**, *46*, 7340–7342.

49 Choi, E.-K.; Jeon, I.-Y.; Bae, S.-Y.; Lee, H.-J.; Shin, H. S.; Dai, L.; Baek, J.-B. High-yield exfoliation of three-dimensional graphite into two-dimensional graphene-like sheets. *Chem. Commun.* **2010**, 6320–6322.

50 Graupner, R.; Abraham, J.; Wunderlich, D.; Vencelova, A.; Lauffer, P.; Roehrl, J.; Hundhausen, M.; Ley, L.; Hirsch, A. Nucleophilic-Alkylation-Reoxidation: A Functionalization Sequence for Single-Wall Carbon Nanotubes. *J. Am. Chem. Soc.* **2006**, *128*, 6683–6689.

51 Wunderlich, D.; Hauke, F.; Hirsch, A. Preferred functionalization of metallic and small-diameter single walled carbon nanotubes via reductive alkylation. *J. Mater. Chem.* **2008**, *18*, 1493–1497.

52 Wunderlich, D.; Hauke, F.; Hirsch, A. Preferred functionalization of metallic and small-diameter single-walled carbon nanotubes by nucleophilic addition of organolithium and -magnesium compounds followed by Reoxidation. *Chem.—Eur. J.* **2008**, *14*, 1607–1614.

53 Syrgiannis, Z.; Gebhardt, B.; Dotzer, C.; Hauke, F.; Graupner, R.; Hirsch, A. Reductive Retrofunctionalization of Single-Walled Carbon Nanotubes. *Angew. Chem., Int. Ed.* **2010**, *49*, 3322–3325.

54 Gebhardt, B.; Syrgiannis, Z.; Backes, C.; Graupner, R.; Hauke, F.; Hirsch, A. Carbon Nanotube Sidewall Functionalization with Carbonyl Compounds-Modified Birch Conditions vs. the Organometallic Reduction Approach. *J. Am. Chem. Soc.* **2011**, *133*, 7985–7995.

55 Gebhardt, B.; Hof, F.; Backes, C.; Mueller, M.; Plocke, T.; Maultzsch, J.; Thomsen, C.; Hauke, F.; Hirsch, A. Selective Polycarboxylation of Semiconducting Single-Walled Carbon Nanotubes by Reductive Sidewall Functionalization. *J. Am. Chem. Soc.* **2011**, *133*, 19459–19473.

56 Rüdorff, W.; Schulze, E. Über Alkaligraphitverbindungen. *Z. Anorg. Allg. Chem.* **1954**, *277*, 156–171.

57 Vallés, C.; Drummond, C.; Saadaoui, H.; Furtado, C. a.; He, M.; Roubeau, O.; Ortolani, L.; Monthioux, M.; Pénicaud, A.; Vallés, C.; Pénicaud, A. Solutions of negatively charged graphene sheets and ribbons. *J. Am. Chem. Soc.* **2008**, *130*, 15802–15804.

58 Catheline, A.; Vallés, C.; Drummond, C.; Ortolani, L.; Morandi, V.; Marcaccio, M.; Iurlo, M.; Paolucci, F.; Pénicaud, A. Graphene solutions. *Chem. Commun.* **2011**, 5470–5472.

59 Englert, J. M.; Dotzer, C.; Yang, G.; Schmid, M.; Papp, C.; Gottfried, J. M.; Steinrück, H.-P.; Spiecker, E.; Hauke, F.; Hirsch, A. Covalent bulk functionalization of graphene. *Nat. Chem.* **2011**, *3*, 279–286.

60 Denisenko, N. I.; Troyanov, S. I.; Popov, A. A.; Kuvychko, I. V.; Žemva, B.; Kemnitz, E.; Strauss, S. H.; Boltalina, O. V. T_h-$C_{60}F_{24}$. *J. Am. Chem. Soc.* **2004**, *126*, 1618–1619.

61 Kelly, K. F.; Chiang, I. W.; Mickelson, E. T.; Hauge, R. H.; Margrave, J. L.; Wang, X.; Scuseria, G. E.; Radloff, C.; Halas, N. J. Insight into the mechanism of sidewall functionalization of single-walled nanotubes: an STM study. *Chem. Phys. Lett.* **1999**, *313*, 445–450.

62 Englert, J. M.; Knirsch, K. C.; Dotzer, C.; Butz, B.; Hauke, F.; Spiecker, E.; Hirsch, A. Functionalization of Graphene by Electrophilic Alkylation of Reduced Graphite. *Chem. Commun.* **2012**, *48*, 5025–5027.